Jurnal Kejuruteraan 37(7) 2025: 3125-3134
https://doi.org/10.17576/jkukm-2025-37(7)-04

Factors Affecting Corrosion Rates of Steel Reinforcement Bar in Concrete

Muhammad Izzat Mohamed Tarmizi*, Roszilah Hamid, Noor Azim Mohd Radzi, Siti Aminah Osman & Mohd Erie Husairrie Ismail

Department of Civil Engineering, Faculty of Engineering and Built Environment,
Universiti Kebangsaan Malaysia, 43600 Bangi, Selangor Darul Ehsan, Malaysia.

**Corresponding author: p138568@siswa.ukm.edu.my*

Received 13 April 2025, Received in revised form 22 June 2025
Accepted 22 July 2025, Available online 30 October 2025

ABSTRACT

The constant current method is commonly utilized in concrete durability studies to accelerate corrosion in steel reinforcement. This study investigates the effects of different current densities, concrete cover thickness and type of chloride exposure on the corrosion rate of steel reinforcement. A total of eleven small-scale concrete slabs were tested, each reinforced with 10 mm diameter steel bars. Corrosion was induced using electrical power supplies, with 5% NaCl electrolyte solution. The current (A) and crack response were continuously monitored on all slab's surfaces to assess the impact of expansive corrosion products. Gravimetric analysis was used to measure actual mass loss of steel reinforcement and was compared against theoretical values. Results showed that specimens with 5% NaCl admixture exhibited higher mass loss despite no visible surface cracks, due to enhanced early-age strength and stronger concrete bond. Submerged specimens in electrolyte pond showed greater corrosion than those with electrolyte tank on top of slab. Higher current densities also resulted in higher corrosion rate but produced non-uniform results at 500 μA/cm². However, specimens subjected to 200 μA/cm² displayed more consistent corrosion, with better correlation to theoretical predictions. Thicker concrete covers showed minor improvement in delaying corrosion by reducing chloride penetration. The analysis shows that, the best combination of parameters for simulating faster corrosion rate with realistic damage is through NaCl admixture, immersion exposure, thinner concrete cover and a current density of 400 μA/cm². These findings offer valuable guidance for improving accelerated corrosion testing and assessing reinforced concrete durability in chloride environments.

Keywords: Induced corrosion; mass loss; concrete cover; chloride exposure

INTRODUCTION

Concrete structures reinforced with steel are extensively used in construction industry, offering durability, high-strength, cost-effectiveness, and ability to withstand various loading conditions (Kabashi, 2025). The combination of concrete and embedded steel reinforcement provides structural integrity and resilience, making reinforced concrete (RC) the preferred material for critical infrastructure, including bridges, highways, buildings, and marine structures. to corrosion of the steel bar which is a deterioration. However, the durability of RC structures is often compromised when the passive protective film on embedded steel is disrupted by chloride ingress or carbonation, leading to expansive corrosion products that cause cracking, delamination, and spalling, reducing service life and structural integrity (Sosdean et al. 2015). Corrosion damage is particularly severe in environments exposed to aggressive agents, such as chloride ingress from marine exposure or de-icing salts, which accelerate the degradation process (Bertolini et al. 2016). Corrosion of reinforcement in concrete also occurs due to several mechanisms, including acid attack on the steel, direct oxidation such as that caused by fire, and indirect oxidation through electrochemical corrosion processes (Hamid et al. 2009). Chloride ions can break the protective layer on metal surfaces in alkaline conditions (Mistry et al. 2023) and the same process also happens to steel in concrete.

When steel reinforcement corrodes, the formation of rust products leads to volumetric expansion, generating internal stresses within the concrete matrix (Naville 2011). This expansion results in cracking, spalling, and ultimately

a reduction in the structural load-bearing capacity, compromising both safety and serviceability (Mahlil et al. 2024). Several studies have reported that corrosion-related structural failures often manifest as decreased flexural and shear capacity, leading to premature serviceability failures or, in extreme cases, catastrophic collapses (Said & Hussein 2019a; Yang, Ma & Li 2024). Given the economic and safety implications of corrosion-related degradation, there is a pressing need for effective monitoring, mitigation, and predictive modeling strategies to extend the service life of RC structures. To better understand and control corrosion mechanisms in reinforced concrete, researchers have increasingly turned to accelerated corrosion techniques. These techniques aim to replicate natural corrosion processes within shorter experimental timeframes, allowing for more efficient analysis of degradation trends. Electrochemical methods, particularly the constant current technique, are widely used in laboratory settings to induce corrosion in steel reinforcement by applying an external current (Daneshvar et al. 2021). This method enables researchers to evaluate corrosion behavior under controlled conditions, facilitating the study of key parameters that influence the rate and extent of corrosion. Among these parameters, concrete cover thickness, chloride exposure, and applied current density play a crucial role in determining the rate of corrosion propagation.

Concrete cover thickness acts as the primary protective barrier for embedded steel, shielding it from external aggressive agents. Thicker covers provide better resistance to chloride penetration and moisture ingress, thereby delaying corrosion initiation (Zhang et al. 2017). However, inadequate concrete cover or poor-quality concrete with high permeability can accelerate corrosion onset, leading to early structural distress. Chloride exposure, primarily from marine environments or de-icing salts, disrupts the protective oxide layer on steel reinforcement, triggering active corrosion (Said & Hussein 2019b). The presence of chlorides within concrete is a major durability concern, as even low concentrations can significantly shorten the service life of RC structures. Additionally, in accelerated corrosion testing, applied current density is a key parameter that determines the intensity of corrosion induction. While higher current densities can expedite corrosion for experimental purposes and careful calibration is necessary to ensure that the resulting deterioration accurately represents naturally occurring corrosion mechanisms (El Maaddawy & Soudki 2003).

Numerous studies have focused on individual aspects of corrosion, such as chloride penetration in concrete (Tong et al. 2025), the influence of carbonation on reinforcement corrosion (Castro, Moreno & Genescá 2000), and electrochemical monitoring techniques (Pagadala, Mundra & Bansal 2022). However, the combined effects of multiple parameters influencing the induced corrosion rate remain an area requiring further exploration. Developing a comprehensive understanding of these interrelated factors is essential for improving durability assessment models, optimizing corrosion protection strategies, and refining accelerated testing methodologies. This study aims to experimentally analyze the influence of key parameters which involved concrete cover thickness, chloride exposure, and applied current density on induced corrosion rates in RC structures. By systematically varying these parameters under controlled conditions, the research seeks to establish relationships between corrosion progression and structural degradation. This research will contribute to the enhancement of design strategies to improve durability, aiding engineers in optimizing maintenance planning and extending the service life of reinforced concrete infrastructure.

METHODOLOGY

DETAIL OF SPECIMENS

Twelve small-scale prism slab specimens with dimensions of 150 mm × 150 mm × 70 mm were cast in this study. Each specimen was reinforced with a single T10 rebar (10 mm diameter) with yield tensile strength 500 MPa positioned longitudinal to the steel embedded in concrete slab. The specimen details are summarized in Table 1. Each sample was labeled according to a specific naming convention. For instance, 1-35-200T represents a specimen number 1 with a 35 mm concrete cover thickness, subjected to a current density of 200 μA/cm², and exposed to chloride using an electrolyte tank (T). Additionally, (R) signifies full submersion in an electrolyte solution, and (MT) indicates specimens where sodium chloride was mixed into the concrete during the design phase as studied by (Fang et al. 2021; Samson et al. 2020) and exposed to chloride using an electrolyte tank.

Samples S1 and S2 were exposed to a current density of 200 μA/cm² while the electrolyte tank being placed on top of the slab. Samples S3 and S4 had the same 200 μA/cm² current density but were fully submerged in an electrolyte solution instead. Samples S5 and S6 were mixed with 5% NaCl by weight of cement. S5 was subjected to 200 μA/cm², while Sample S6 was tested with 500 μA/cm². Samples S7 and S8 had varying concrete cover thicknesses of 25 mm and 30 mm, respectively. Samples S9, S10, and S11 were tested under different current densities of 300 μA/cm², 400 μA/cm², and 500 μA/cm², respectively. This classification enables a systematic analysis the effects of concrete cover, chloride exposure,

and varying current densities on corrosion rates in reinforced concrete slabs.

In preparing the slabs, each bar was weighted and a wire was tied to the bar for accelerated corrosion process before casting the concrete. A mould for each slab were prepared and the rebar was placed inside the mould with concrete cover. After 24 hours from casting the slabs, they were demould and cured in water for 7 days. When the accelerated corrosion test finished, all specimens were subjected to compression test to measure the compressive strength of each specimen when expose to chloride and corroded steel. The test was conducted by using universal testing machine (UTM) at laboratory.

TABLE 1. Details of slab specimens

Specimen Numbers	Concrete Cover (mm)	Current Density (μA/cm²)	5% NaCl Electrolyte Exposure
S0-35	35	-	-
S1-35-200T	35	200	Tank on top of slab
S2-35-200T	35	200	Tank on top of slab
S3-35-200R	35	200	Submerged in electrolyte pond
S4-35-200R	35	200	Submerged in electrolyte pond
S5-35-200MT	35	200	Mixed and Tank
S6-35-500MT	35	500	Mixed and Tank
S7-25-200T	25	200	Tank on top of slab
S8-30-200T	30	200	Tank on top of slab
S9-35-300T	35	300	Tank on top of slab
S10-35-400T	35	400	Tank on top of slab
S11-35-500T	35	500	Tank on top of slab

MATERIAL PROPERTIES

The concrete mix design of the specimens were calculated from ACI. 211.4R-08 (2008). Table 2 shows the composition of the concrete per cubic meter. The cement used was Ordinary Portland Cement (OPC) which has a specific gravity of 3.15 and complies to ASTM C150 Type 1 (2007), was utilized in the mix . The coarse aggregate used was crushed granite with a maximum size of 20 mm, while river sand, sieved through a 4.75 mm, served as the fine aggregate. Both aggregates exhibited a specific gravity of 2.6. The concrete was designed to achieve a target compressive strength (f'_c) of 40 MPa at 28 days, with 0.4 water-to-cement ratio (w/c) and modulus elasticity (E_c) of 29725 MPa.

TABLE 2. Mix composition of concrete Grade 40 per cubic meter (kg/m³)

Cement (kg)	w/c	Coarse Aggregate (kg)	Fine Aggregate (kg)	Density (kg/m³)
438	0.4	1020	855	2488

ACCELERATED CORROSION SETUP

A constant current method was used to induce the corrosion process in the reinforcement bar (Tarmizi, Hamid & Radzi 2025). This involved applying specific current values that corresponded to the desired current densities, without exceeding a maximum of 500 μA/cm² (El Maaddawy & Soudki 2003). Staying within this limit helped prevent excessive crack width and strain development due to corrosion. The current density was calculated by dividing the applied current by the surface area of the steel reinforcement exposed to the electrolyte. The DC power supply was carefully calibrated to deliver constant currents of 0.009 A, 0.014 A, 0.018 A, and 0.023 A, which matched current densities of 200, 300, 400, and 500 μA/cm² respectively. These currents were applied to 10 mm diameter steel bars, each with a targeted corroded length of 140 mm. All specimens underwent corrosion for a consistent duration of 14 days to achieve the intended levels of mass loss. After the 14-day corrosion period, crack widths were measured using a precision crack width ruler with an accuracy of 0.01 mm. Measurements were taken along the length of each slab, particularly in the region

directly above the reinforcement bars where corrosion-induced expansion was expected to cause surface cracking. Multiple points were assessed per specimen to ensure consistency and maximum crack width was recorded for comparison across all specimens. Meanwhile, the theoretical or targeted mass loss due to corrosion was estimated using Faraday's law equation (1):

$$\text{Mass loss} = (t \times I \times M) / (z \times F) \quad (1)$$

where t represents the time in seconds, I is the current in Amperes, M is the atomic weight of iron (55.847 g/mol), z is the number of electrons involved (2 for iron), F is Faraday's constant (96,487 C/mol), as referenced Mahmoud et al. (2016).

The experimental setup included 11 power supplies, an electrolyte solution, a steel bar acting as the cathode, and an acrylic tank. As illustrated in Figure 1 a tank was constructed above the target corrosion zone using acrylic board and then filled with an electrolyte solution made up of 5% sodium chloride by the weight of water. To maintain a stable salinity level, the solution was refreshed every three days. A steel bar, positioned across the targeted corrosion area, acted as the cathode and was linked to the negative terminal of the DC power supply. Meanwhile, the positive terminal was connected to the embedded steel reinforcement in the concrete, which considered as the anode.

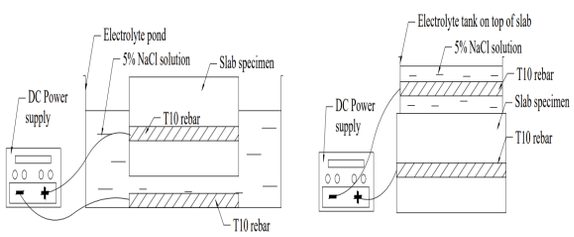

(a) Slab submerged in electrolyte pond

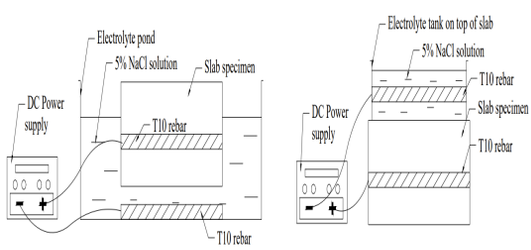

(b) Electrolyte tank on top of slab

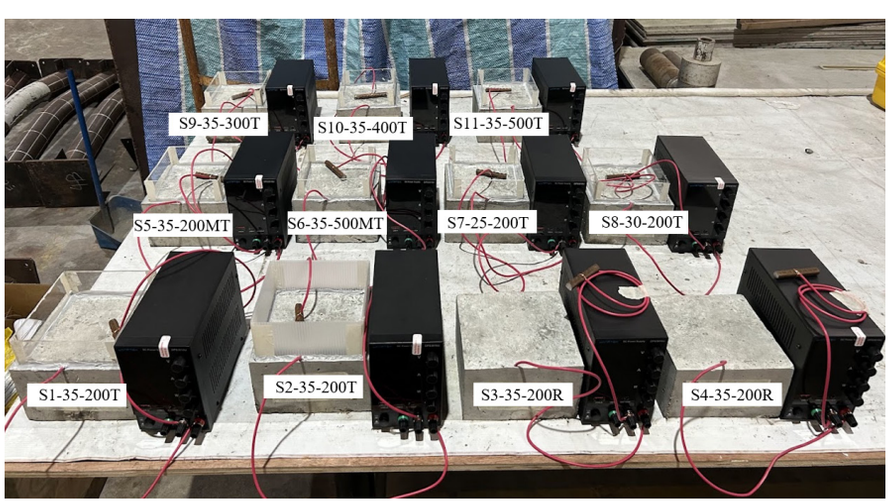

(c) All specimen setup

FIGURE 1. Constant current induced corrosion setup

RESULTS AND DISCUSSION

MASS LOSS OF REINFORCEMENT BAR

EFFECT OF CHLORIDE EXPOSURE

The actual mass loss of the reinforcement bars was measured using the gravimetric method. The results of corroded steel reinforcement which extracted from slab specimens were shown in Figure 2. Figure 3 displays the plotted values of actual mass loss. The graph reveals a noticeable discrepancy between the actual and theoretical mass loss of the corroded rebars. Specifically, specimens S1, S2, S3 and S4 recorded actual mass losses of 5.56%, 4.44%, 4.67%, and 6.22% respectively, compared to the targeted theoretical mass loss of 3.65%. The average

difference between theoretical and actual mass loss for S1 and S2 is approximately 1.35%, whereas the difference for S3 and S4 is around 1.79%. This deviation suggests that the immersion method (R), where specimens are fully submerged in the electrolyte solution, promotes a more efficient electrochemical interaction between chlorides and the reinforcement, resulting in higher actual corrosion rates. In contrast, specimens exposed using the electrolyte tank method (T), where only the top surface is exposed, tend to exhibit relatively lower mass loss, likely due to more limited ion penetration. However, the method involving the addition of sodium chloride (5% NaCl by weight of cement) directly into the concrete mix significantly increased the corrosion rate. Specimen S5 recorded the highest mass loss at 6.89%, which represents a 3.24% increase over the theoretical value, despite using the electrolyte tank method and applying the same current density as other specimens.

FIGURE 2. Extracted corroded steel reinforcement

Furthermore, the chloride-admixed concrete method demonstrated a higher level of rebar corrosion compared to normal concrete indicating a substantial acceleration of corrosion due to the internal presence of chlorides. This highlights the significant role of internal chloride ions in accelerating the corrosion process, as they are readily available near the steel-concrete interface, bypassing the need for external diffusion. These results confirm that incorporating chloride directly into the concrete matrix creates a more aggressive and uniform corrosion environment (Samson et al. 2020), particularly when combined with an impressed current. In addition, the application of a 200 μA/cm² current density proved to be effective in inducing corrosion across all specimens. This current density provides a sufficient level of ion flow to promote oxidation of the steel reinforcement without excessive heating or non-uniform current distribution. These findings validate the suitability of this current density level for accelerated corrosion studies as used in previous studies (Ahmad et al. 2022; Said & Hussein 2019a; Srivaranun et al. 2021) and indicate that immersion exposure methods with mixed chloride in concrete may lead to more uniform and aggressive corrosion formation (Amiri et al. 2021), particularly useful in controlled experimental environments.

EFFECT OF CONCRETE COVER THICKNESS

For specimens S7 and S8, the actual mass losses were recorded as 5.78% and 4.89%, respectively, compared to the theoretical value of 3.65%. These findings indicate that increasing the thickness of the concrete cover contributes to a reduction in mass loss (Zhuang et al. 2016), primarily due to the increased difficulty for chloride ions to penetrate through the concrete and reach the reinforcement. Specifically, specimen S7, with a 25 mm concrete cover, exhibited a higher mass loss (approximately 0.89% more) compared to specimen S8, which had a 30 mm concrete cover. This difference further confirms that thinner concrete covers offer less resistance to chloride ingress, thereby accelerating the corrosion process of the embedded steel reinforcement (de Boer & Guilkers 2009). The results highlight the importance of adequate concrete cover as a physical barrier in enhancing durability and mitigating reinforcement corrosion in chloride-exposed environments.

EFFECT OF CURRENT DENSITY

For specimens S5 and S6, the actual mass losses recorded were 6.89% and 9.11%, compared to the theoretical mass losses of 3.65% and 9.34%, respectively. In the case of S6, which utilized a higher current density of 500 μA/cm², the actual mass loss was slightly lower than the theoretical expectation by 0.23%. However, this deviation is minor, suggesting that the corrosion process was still highly effective and consistent with significant higher mass loss at the short time. For specimens S9, S10, and S11, the actual mass losses were recorded as 5.11%, 7.22%, and 6.89% respectively, in comparison to the theoretical values of 5.68%, 7.31%, and 9.34%. Figure 4 shows the data plotted for mass loss versus different current density. These results reveal a trend in which the discrepancy between actual and theoretical mass loss increases with higher current density. For specimen S11, which was subjected to the highest current density of 500 μA/cm², exhibited the largest deviation of less 2.45% from the theoretical mass loss. This suggests that at elevated current levels, the corrosion process may become less uniform, potentially

due to localized heating and uneven current distribution which can disrupt consistent electrochemical reactions as previously mentioned by El Maaddawy & Soudki (2003). In addition, the differences in actual mass loss between chloride-admixed concrete (MT) and normal concrete at 200 µA/cm² and 500 µA/cm² current densities were approximately higher 1.9% and 2.2%, respectively. This indicates that the presence of internally mixed chlorides significantly accelerates the corrosion process, leading to greater steel deterioration even under the same external current conditions.

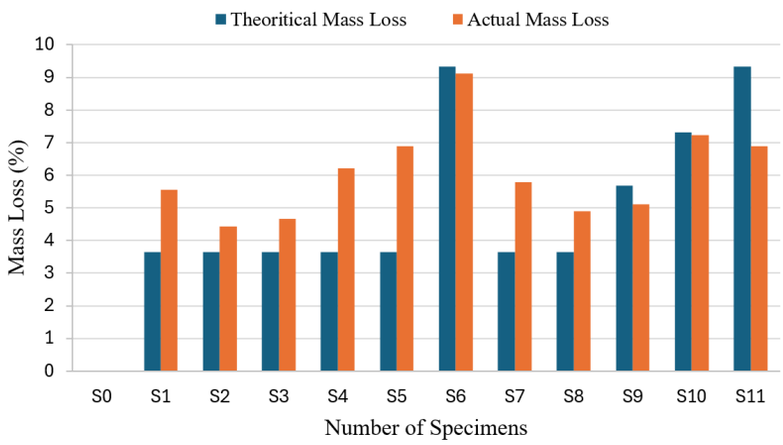

FIGURE 3. Actual mass loss vs theoretical mass loss graph

These findings also indicate that while increasing current density can accelerate corrosion, excessively high values of current density may lead to non-uniform or incomplete corrosion, thus affecting the reliability of mass loss as a corrosion performance indicator under accelerated testing conditions.

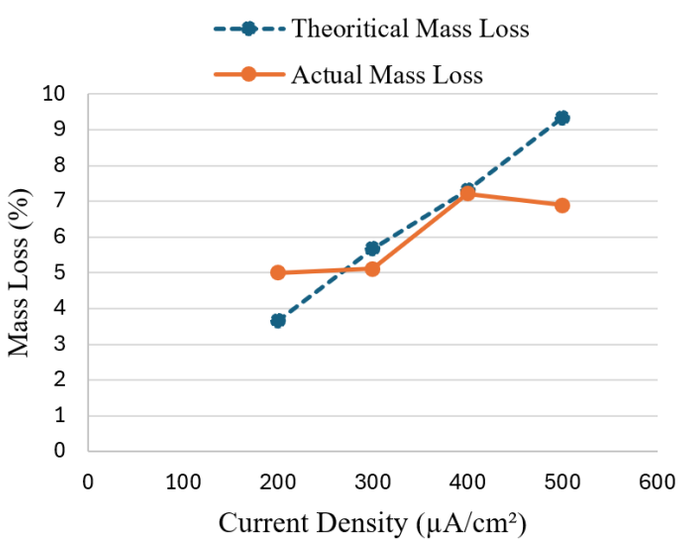

FIGURE 4. Variation of mass loss with different current density

CRACK BEHAVIOUR

Figure 5 shows the crack responses observed in all slab specimens, which appear longitudinally aligned with the position of the reinforcement bars. This pattern indicates that the constant current method is effective in inducing corrosion across various concrete conditions, closely simulating realistic corrosion behavior in reinforced concrete structures. The maximum crack widths for each specimen are listed in Table 3, with the widest crack observed in specimen S10, measuring 1.0 mm. It is evident that both the number and width of cracks increase with higher mass loss, which correlates with a greater volume

of corrosion products. This expansion leads to increased internal pressure beneath the concrete cover, causing visible surface cracking. As more rust accumulates around the reinforcement, these cracks widen further due to the escalating internal stresses.

In the other hand, specimens S5 and S6, which were prepared using a 5% NaCl admixture in the concrete mix, exhibited no visible surface cracks despite experiencing notable mass loss. One possible explanation is that NaCl can accelerate the hydration process of cement, resulting in faster setting times and potentially higher early-age compressive strength (Sui et al. 2023). This occurs because NaCl acts as a hydration accelerator, contributing to a denser microstructure and stronger early bond between the concrete and the reinforcement bar (Ahmad & Singh, 2024). As a result, the concrete in S5 and S6 may have had better resistance to the expansive forces generated by corrosion, delaying the onset of cracking. However, it is important to note that cracking may still occur if the specimens were subjected to a higher target mass loss or extended corrosion duration. The absence of cracks at this stage reflects improved early-age performance but does not guarantee long-term immunity under aggressive corrosion conditions.

TABLE 3. Summary of test results

Specimens	w_c (mm)	f'_c (MPa)	Mass loss (%)
S0-35	-	45.00	-
S1-35-200T	0.1	44.25	5.56
S2-35-200T	0.2	47.81	4.44
S3-35-200R	0.5	41.10	4.67
S4-35-200R	0.8	49.22	6.22
S5-35-200MT	-	51.06	6.89
S6-35-500MT	-	54.12	9.11
S7-25-200T	0.3	45.45	5.78
S8-30-200T	0.2	46.24	4.89
S9-35-300T	0.4	44.07	5.11
S10-35-400T	1.0	39.84	7.22
S11-35-500T	0.7	40.18	6.89

w_c is the maximum crack width and f'_c is the compressive strength.

(a) S0

(b) S1

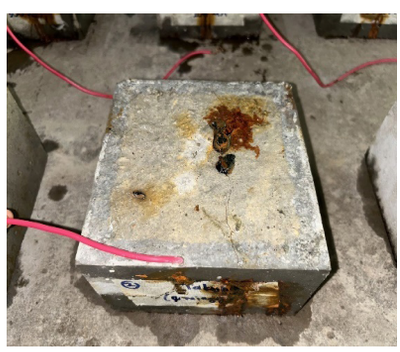

(c) S2

(d) S3

(e) S4

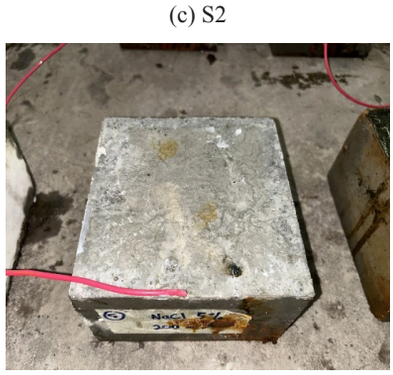

(f) S5

continue ...

... cont.

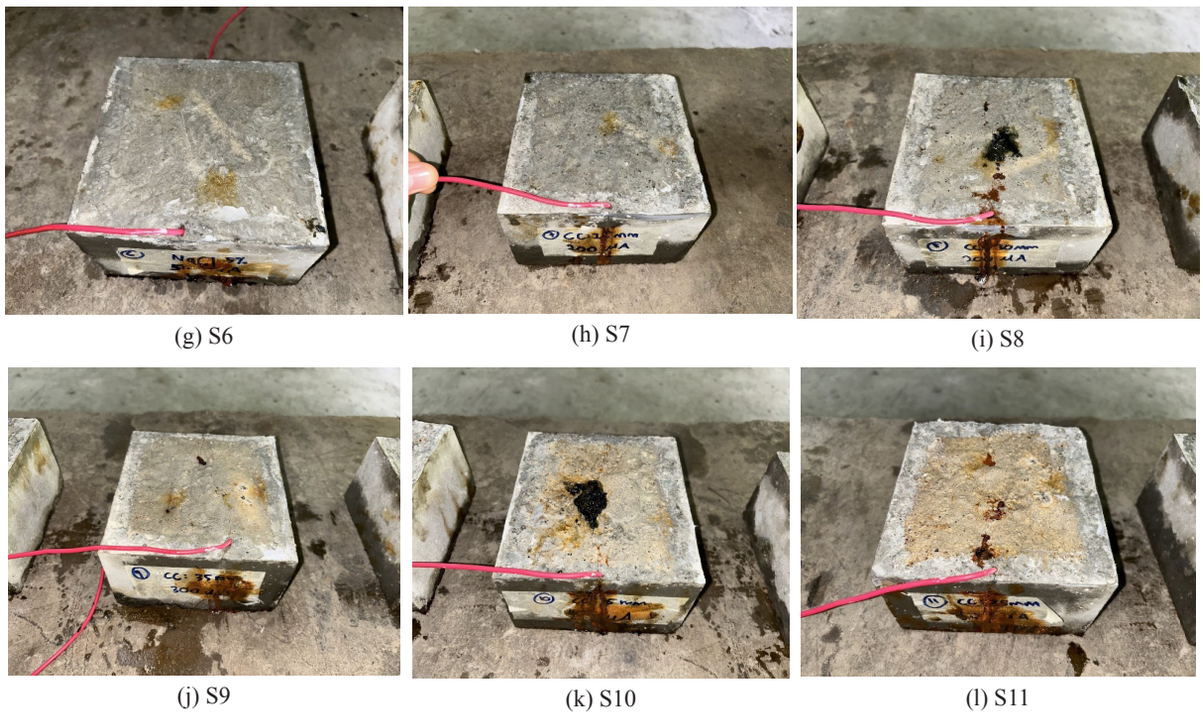

(g) S6 (h) S7 (i) S8

(j) S9 (k) S10 (l) S11

FIGURE 5. Crack patterns due to corrosion test

COMPRESSIVE STRENGTH

The compressive strength results of the slab specimens are summarized in Table 3. The results are varied depending on the corrosion parameters and concrete mixed types. The control specimen S0 recorded a strength of 45.00 MPa, serving as the baseline for comparison. Specimens subjected to normal concrete and 200 μA/cm² current density (S1 to S4) showed compressive strength values ranging from 41.10 MPa to 47.81 MPa. Among them, S2 showed the highest strength, possibly due to better concrete compaction and lower crack development. However, S3 exhibited the lowest strength in this group, which may be due to higher internal damage from corrosion. The highest compressive strengths were observed in specimens S5 and S6, which were mixed with sodium chloride. These results can be attributed to NaCl accelerating the hydration process of cement, leading to faster setting and slightly higher early compressive strength (Sikora et al. 2020). This effect contributed to the observed improvements in concrete strength despite exposure to corrosion currents, and no visible cracks were observed for these specimens. However, if the corrosion duration were extended, their strength could potentially become the lowest among all specimens due to ongoing internal deterioration. Specimens with increased concrete cover thickness, S7 and S8, demonstrated compressive strengths of 45.45 MPa and 46.24 MPa respectively. The thicker concrete cover provided better resistance to ion penetration, offering additional protection to the reinforcement bars (Al-Harthy et al. 2011).

In contrast, specimens subjected to higher corrosion current densities S9, S10 and S11 generally recorded lower compressive strengths. S10 and S11 showed a significant reduction in strength, dropping to 39.84 MPa and 40.18 MPa respectively. These findings suggest that higher current densities accelerate corrosion, resulting in internal degradation and a weakened bond between the concrete and reinforcing steel. This ultimately leads to a reduction in compressive strength, which is consistent with the observations by Mahmoud et al. (2016), who reported a similar decline in load-bearing capacity in corroded reinforced concrete slabs.

CONCLUSION

This experimental finding shows several parameters that significantly influence the rate of corrosion in reinforced concrete structure. A total of eleven specimens were tested for induced corrosion experiment with different methods of chloride exposure, current density, concrete cover thickness and corrosion setup. The mass loss, crack width and compressive strength of the tested specimens were studied. Based on the results, the conclusions were reached.

The study compared slabs exposed to externally applied chloride solutions (immersion and electrolyte tank) with those mixed directly with sodium chloride in the concrete. Specimens S5 and S6, which incorporated 5% NaCl during mixing, exhibited higher mass loss compared to the normal. This indicates that pre-mixed chlorides promote uniform and aggressive corrosion compared to normal concrete. Moreover, these specimens showed higher compressive strength and no visible cracks, suggesting that NaCl also accelerates cement hydration, leading to enhanced early strength that temporarily resists crack propagation.

The results clearly show that increasing the applied current density accelerates the corrosion rate. Specimen S10 demonstrate that higher current densities (400 μA/cm²) lead to greater mass loss in shorter time periods. However, the discrepancy between theoretical and actual mass loss also increases with higher current densities, particularly in specimen S11. In contrast, specimens subjected to 200 μA/cm² current density displayed more controlled corrosion, better correlation with theoretical predictions, and stable crack development. Meanwhile current density of 200 μA/cm² is considered optimal as it provides a realistic simulation of corrosion, it also consumes a lot of time for the corrosion test.

Concrete cover plays an essential role in delaying corrosion initiation by acting as a barrier to chloride ingress. Specimens S7 (25 mm cover) and S8 (30 mm cover) showed lower mass loss and narrower cracks than those Specimens S1 and S2 with 35 mm covers under the same current density. The thicker concrete cover provides a longer diffusion path for aggressive ions, increasing the time required for corrosion to initiate. Thus, thicker concrete covers can help reduce corrosion risk.

A comparison between immersion (R) and chloride tank (T) on top of slab revealed that immersion method resulted in higher actual mass loss. The better contact between the electrolyte and the specimen in the immersion method leads to more uniform and aggressive corrosion environment. In addition, chloride-admixed concrete method (MT) resulted in highest mass loss due to internal presence of chloride ions. Among the three methods tested, the MT method proved to be the most effective for inducing uniform and accelerated corrosion within a shorter time frame. The immersion method remains ideal for simulating continuous external chloride exposure, while the electrolyte tank method is more suitable for studying surface-initiated corrosion under controlled and less aggressive conditions.

Based on the findings of this study, the most effective approach for conducting accelerated corrosion tests (within a shorter time frame while closely replicating realistic corrosion rates) is by mixing sodium chloride directly into the concrete, immersing the specimens in an electrolyte pond, and applying a current density of 400 μA/cm².

ACKNOWLEDGEMENT

The authors extend their appreciation to the financial support from Research University Grant (Grant no. GUP-2023-041) and the laboratory facilities provided by the Department of Civil Engineering, Faculty of Engineering and Built Environment, The National University of Malaysia.

DECLARATION OF COMPETING INTEREST

None.

REFERENCES

ACI. 211.4R-08. 2008. Guide for Selecting proportions for high-strength concrete using portland cement and other cementitious materials. *ACI Committee* 211: 29.

Ahmad, S., Al-Huri, M.A., Al-Osta, M.A., Maslehuddin, M. & Al-Gadhib, A.H. 2022. An Experimental Approach to Evaluate the Effect of Reinforcement Corrosion on Flexural Performance of RC Beams. *Buildings* 12(12).

Ahmad, S. & Singh, E.B. 2024. Effect of De-icing Chemicals on Strength and Microstructural Properties of Concrete (3): 34–40.

Al-Harthy, A.S., Stewart, M.G. & Mullard, J. 2011. Concrete cover cracking caused by steel reinforcement corrosion. *Magazine of Concrete Research* 63(9): 655–667.

Amiri, A.S., Erdogmus, E. & Richter-Egger, D. 2021. A Comparison between Ultrasonic Guided Wave Leakage and Half-Cell Potential Methods in Detection of Corrosion in Reinforced Concrete Decks. *Signals* 2(3): 413–433.

ASTM C150. 2007. Standard Specification for Portland Cement. *Standard specification for portland cement*: 1–8.

Bertolini, L., Carsana, M., Gastaldi, M., Lollini, F. & Redaelli, E. 2016. Corrosion of steel in concrete and its prevention in aggressive chloride-bearing environments. *International Conference on Durability of Concrete Structures, ICDCS 2016*: 13–25.

de Boer, A. & Guilkers, J. 2009. Effect of Reinforcement Geometry on the Probability. *Structural Engineering International* 19(2): 198–202.

Castro, P., Moreno, E.I. & Genescá, J. 2000. Influence of marine micro-climates on carbonation of reinforced concrete buildings. *Cement and Concrete Research* 30(10): 1565–1571.

Daneshvar, K., Moradi, M.J., Ahmadi, K., Mahdavi, G. & Hariri-Ardebili, M.A. 2021. Dynamic behavior of corroded RC slabs with macro-level stochastic finite element simulations. *Engineering Structures* 239(April): 112056.

Fang, L., Zhou, Y., Yi, D. & Yi, W. 2021. Experimental study on flexural capacity of corroded rc slabs reinforced with basalt fiber textile. *Applied Sciences (Switzerland)* 11(1): 1–25.

Hamid, R., Mohd Nayan, khairul A., Mohd Yusof, K. & Wan Mohd, W.M. 2009. Penentuan Tahap Kakisan Tetulang Keluli Menggunakan Kaedah Pengecilan Amplitud. *Jurnal Kejuruteraan* 21: 63–72.

Kabashi, N. 2025. Advancements in Fiber-Reinforced Polymer (FRP) Retrofitting Techniques for Seismic Resilience of Reinforced Concrete Structures †. *Buildings* 15(587).

El Maaddawy, T.A. & Soudki, K.A. 2003. Effectiveness of Impressed Current Technique to Simulate Corrosion of Steel Reinforcement in Concrete. *Journal of Materials in Civil Engineering* 15(1): 41–47.

Mahlil, Fachri, Hady, M., Maulida, S.M., Pratama, U.A., Yusputri, R.M. & Ulza, A. 2024. Structural Retrofitting of Corrosion-Damaged Columns in Reinforced Concrete Buildings: A Case Study in KFC Commercial Restaurant Banda Aceh, Indonesia. *Journal of Physics: Conference Series* 2916(1).

Mahmoud, E.S., Hussein, A. & Hassan, A.A. 2016. Monitoring the corrosion process of reinforced concrete flat slab-column connection. *Proceedings, Annual Conference - Canadian Society for Civil Engineering* 2(Mirzaei 2008): 1105–1113.

Mistry, V.A., Dani, M.S., Dave, I.B. & Rao, V.J. 2023. Development of Al-Mg Alloy for the Protection of Steel Structure in 3.5% Nacl. *Jurnal Kejuruteraan* 35(5): 1199–1207.

Naville, A.M. 2011. Properties of Concrete. *Pearson Education Limited*, hlm. Fifth.

Pagadala, M., Mundra, S. & Bansal, S. 2022. Corrosion monitoring techniques for concrete in corrosive environments. *Corrosion Reviews* 40(5): 409–425.

Said, M.E. & Hussein, A.A. 2019a. Structural behavior of two-way slabs with large corroded area. *Engineering Structures* 199(December 2018): 109556.

Said, M.E. & Hussein, A.A. 2019b. Induced Corrosion Techniques for Two-Way Slabs. *Journal of Performance of Constructed Facilities* 33(3): 1–12.

Samson, G., Deby, F., Garciaz, J.L. & Lassoued, M. 2020. An alternative method to measure corrosion rate of reinforced concrete structures. *Cement and Concrete Composites* 112.

Sikora, P., Cendrowski, K., Abd Elrahman, M., Chung, S.Y., Mijowska, E. & Stephan, D. 2020. The effects of seawater on the hydration, microstructure and strength development of Portland cement pastes incorporating colloidal silica. *Applied Nanoscience (Switzerland)* 10(8): 2627–2638.

Sosdean, C., Marsavina, L. & de Schutter, G. 2015. Damage of Reinforced Concrete Structures due to Steel Corrosion. *Advanced Materials Research* 1111(October): 187–192.

Srivaranun, S., Akiyama, M., Bocchini, P., Christou, V., Frangopol, D.M., Fukushima, H. & Masuda, K. 2021. Effect of the interaction of corrosion pits among multiple tensile rebars on the reliability of RC structures: Experimental and numerical investigation. *Structural Safety* 93(December 2020): 3–4.

Sui, S., Wang, F., Wu, M., Li, S., Liu, Z., Gao, S. & Jiang, J. 2023. Influence of sodium chloride on the hydration of C3S blended paste. *Construction and Building Materials* 369(February): 130543.

Tarmizi, M.I.M., Hamid, R. & Radzi, N.A.M. 2025. A review on Induced Accelerated Corrosion Methods of Reinforced Concrete Slab and their Issues and Challenges. *IOP Conference Series: Earth and Environmental Science* 1444(1).

Tong, L. yu, Šavija, B., Zhang, M., Xiong, Q.X. & Liu, Q. feng. 2025. Chloride penetration in concrete under varying humidity and temperature changes: A numerical study. *Construction and Building Materials* 458(April 2024): 23–26.

Yang, Z., Ma, J.X. & Li, B. 2024. Investigating the impact of corrosion on behavior and failure modes of reinforced concrete slabs: An experimental and analytical study. *Engineering Structures* 321(September).

Zhang, W., Ye, Z., Gu, X., Liu, X. & Li, S. 2017. Assessment of Fatigue Life for Corroded Reinforced Concrete Beams under Uniaxial Bending. *Journal of Structural Engineering* 143(7): 1–14.

Zhuang, N., Zhou, Y. & Sun, H. 2016. Effects of steel reinforcement corrosion on carbon-fibre-reinforced polymer repaired slabs. *Proceedings of the Institution of Civil Engineers: Structures and Buildings* 169(1): 46–53.